

Early-Warning Signs for Pattern-Formation in Stochastic Partial Differential Equations

Karna Gowda* and Christian Kuehn†

March 25, 2014

Abstract

There have been significant recent advances in our understanding of the potential use and limitations of early-warning signs for predicting drastic changes, so called critical transitions or tipping points, in dynamical systems. A focus of mathematical modeling and analysis has been on stochastic ordinary differential equations, where generic statistical early-warning signs can be identified near bifurcation-induced tipping points. In this paper, we provide some basic steps to extend this theory to stochastic partial differential equations. In particular, we study stochastic versions of the Swift-Hohenberg and Ginzburg-Landau equations. We derive a scaling law of the covariance operator in a regime where linearization is expected to be valid. We compare these results to direct numerical simulation, and study the influence of noise level, noise color, distance to bifurcation and domain size on early-warning signs.

1 Introduction

Drastic sudden changes in dynamical systems, so called critical transitions or tipping points, occur in a wide variety of applications. It is often desirable to find early-warning signs to anticipate transitions in order to avoid or mitigate their effects [74]. There has been tremendous recent progress in determining potential warning signs in various sciences such as ecology [76, 80], climate science [58, 59], engineering [21, 61], epidemiology [55, 67], biomedical applications [65, 81] and social networks [54]; see also [73, 75] for concise overviews. For a large class of critical transitions, the underlying dynamical mechanism involves a slow drift of a system parameter towards a local bifurcation point, where a fast transition occurs [50]. This class has been denoted

*Engineering Sciences and Applied Mathematics, Northwestern University, Evanston, IL 60208-3125, USA

†Institute for Analysis and Scientific Computing, Vienna University of Technology, 1040 Vienna, Austria

“B-tipping” in [2]. A detailed mathematical analysis of the underlying stochastic fast-slow systems, including their generic scaling laws, can be found in [52]; see also [5] for further mathematical background.

An example warning sign occurring in many stochastic systems is an increase in variance as a bifurcation point is approached [16]. This effect is intrinsically generated by critical slowing down (or “intermittency” [37]), i.e. the underlying deterministic dynamics becoming less stable near the bifurcation point. Hence, (additive) stochastic fluctuations become dominant approaching a B-tipping point.

A substantial effort has been made to extract early-warning signs, such as slowing down and variance increase, from univariate time series e.g. using various time series analysis methods [40, 60, 62], normal forms [78], topological methods [7] and generalized models [57]. Although theoretical tests and models with sufficiently large data sets tend to work very well [24, 52], there are clear limits to predictability [13], particularly when relatively sparse data sets are considered [18, 26, 28, 56].

For systems with spatio-temporal dynamics (and associated spatio-temporal data), the additional data in the spatial direction may be used to improve existing early-warning signs and to discover new ones. If a system is initialized in a spatially patterned state instead of a homogeneous one, then one could try to consider measures of the pattern as potential candidates to provide warning signs. For example, in [47] patchiness of states in a vegetation model is used. However, for a uniform homogeneous steady state that undergoes a bifurcation, such warning signs are not expected to be available.

Many early-warning signs computed for univariate time series have multivariate time series analogs, such as spatial variance and skewness [29, 38] as well as slowing down and spatial correlation [25]. An “averaging” over the spatial direction, e.g. in the sense of the Moran coefficient [27], can be helpful to facilitate direct comparisons with univariate indicators. Also, a natural alternative to avoid the full complexity of spatial temporal pattern formation is to focus on early-warning signs for traveling waves [53]. Despite these exploratory works, it is quite clear at this point that the full mathematical analysis of early-warning signs for stochastic spatio-temporal systems is largely uncharted territory.

For finite-dimensional B-tipping, a quite robust classification scheme [2, 50] has been formulated and associated warning signs have been investigated (for up to generic codimension-two bifurcations) based upon normal forms, fast-slow systems and stochastic analysis [52]. Such a detailed scheme is unlikely to be possible for spatio-temporal systems since there is no complete generic theory for all spatio-temporal systems available. However, it is expected that certain subclasses of stochastic partial differential equations (SPDEs) have warning-signs near pattern-forming bifurcations that can be studied in detail. For deterministic partial differential equations (PDEs), quite a number of bifurcations leading to pattern-formation are well studied; for example, see [22, 23, 44] and references therein.

Translating and extending the *qualitative* pattern-forming results from PDEs to SPDEs is an extremely active area of current research. We refer for additional background and references to [9, 33]. However, when searching for early-warning signs, it is important to augment the qualitative results with quantitative scaling laws.

Although the problem of early-warning signs for spatio-temporal systems is discussed often¹, there is no complete mathematical theory available to address how classical early-warning signs can be generalized from stochastic ordinary differential equations (SODEs) to SPDEs. In this paper, we limit ourselves to a several elementary steps working toward this generalization:

- We review the available literature from various fields. In particular, there are closely related contributions from statistical physics, dynamical systems, stochastic analysis, theoretical ecology and numerical analysis.
- We outline the basic steps to generalize classical SODE warning signs, such as autocorrelation and variance increase, to the spatio-temporal setting for two standard models for pattern formation, the Swift-Hohenberg (SH) equation and the Ginzburg-Landau (GL) equation.
- We numerically investigate the SH and GL equation to connect back to several spatio-temporal warning signs proposed in applications, particularly in the context of ecological models.
- The numerical results reveal two interesting scaling regimes. Furthermore, we obtain results about the influence of several natural parameters (domain size, distance to bifurcation, noise level and noise correlation length) on early-warning signs.

This paper is structured as follows: In Section 2, we summarize the relevant background for the SH and GL PDEs. We also recall some basic techniques for studying SPDEs, with a focus on the relationship between correlation functions and Q-Wiener processes used to define the spatio-temporal noise. In Section 3, we analytically investigate the covariance operator of the linearized SPDE to capture behavior in the regime in which we expect to observe the first warning signs of an approaching bifurcation-point. Here, we find a very natural generalization to SPDEs of the SODE variance-increase as an early-warning sign. In Section 4, we summarize the measures we compute for the numerical investigation of SPDE early-warning signs in Section 5. In particular, we use numerical simulation results of the SH and GL SPDEs to illustrate the analytical scaling laws and to link our results to several warning signs proposed recently in applications. Another purpose for the numerical simulations is to understand the influence of several system parameters. Appendix A provides an overview of the numerical methods we used. Section 6 provides a brief outlook of possible future work.

¹For example, at the two recent workshops: (I) “Critical Transitions in Complex Systems” at Imperial College London, 19 March–23 March, 2012; (II) “Tipping points: fundamentals and applications” at ICMS Edinburgh, 9 September–13 September, 2013.

2 The Setup

In this section, we review the background required for the proceeding sections. For the review of deterministic PDEs, we briefly state the main results, omitting many details. The theory needed for our example PDEs, the SH and GL equations, is quite well-established. The stochastic analysis is less well-known, and we shall thus explain a bit more for the review of SPDEs.

2.1 The Deterministic PDE(s)

We focus on the one-dimensional spatial case on a bounded domain and use the notation

$$\mathcal{I} := [0, L], \quad (x, t) \in \mathcal{I} \times [0, T] \quad \text{and} \quad u = u(x, t) \in \mathbb{R}.$$

Let X be a (complex) Hilbert space with inner product denoted by $\langle \cdot, \cdot \rangle$. Let $A_{(\cdot)} : D(A_{(\cdot)}) \subset X \rightarrow X$ be a linear operator with a dense domain $D(A_{(\cdot)})$. Assume $A_{(\cdot)}$ is the infinitesimal generator of a strongly continuous semigroup $S(t)$ [69]; the subscript, indicated via the placeholder (\cdot) distinguishes the two differential operators we consider below. For functions $v : \mathcal{I} \rightarrow \mathbb{R}$, we use the standard notation for Sobolev spaces and consider the norm

$$\|v\|_{W^{k,p}(\mathcal{I})}^p := \sum_{\alpha=0}^k \int_{\mathcal{I}} |(D_x^\alpha v)(y)|^p dy,$$

for $p \in [1, \infty)$, $k \in \mathbb{N}_0 = \{0, 1, 2, \dots\}$, and $D_x^\alpha = \frac{\partial^\alpha}{\partial x^\alpha}$ is understood as a weak derivative when the norm $\|v\|_{W^{k,p}(\mathcal{I})}$ is considered. We then denote

$$W^{k,p}(\mathcal{I}) := \{v : \|v\|_{W^{k,p}(\mathcal{I})} < \infty\}, \quad H^k(\mathcal{I}) := W^{k,2}(\mathcal{I}), \quad L^p(\mathcal{I}) := W^{0,p}(\mathcal{I}).$$

Mirroring the finite-dimensional classification scheme for B-tipping [52], we specify a class of deterministic systems of the form

$$\partial_t u = Au + f(u) = ru + A_{(\cdot)}u + f(u), \quad (1)$$

where $f(u) = f(u(x, t))$ is a sufficiently smooth polynomial nonlinearity with $f : \mathbb{R} \rightarrow \mathbb{R}$, $A := A_{(\cdot)} + r \text{Id}$ is a linear operator and we use the shorthand notation $\partial_t = \frac{\partial}{\partial t}$.

The primary example of (1) we consider in this paper is the Swift-Hohenberg (SH) equation [77]

$$\partial_t u = r_{\text{SH}}u - (1 + \partial_x^2)^2 u - u^3, \quad (2)$$

where $r_{\text{SH}} \in \mathbb{R}$ is a parameter and $A_{\text{SH}} := -(1 + \partial_x^2)^2$ is defined on a suitable domain that is dense in the Hilbert space $X = L^2(\mathcal{I})$ (we employ the notation $\partial_x^2 = \frac{\partial^2}{\partial x^2}$). It can be verified that A_{SH} generates an analytic semigroup under mild conditions. For periodic boundary conditions, there is a convenient set of orthonormal eigenfunctions of A_{SH} given by $a_k^{\text{SH}}(x) = \frac{1}{L} \exp\left(\frac{2\pi i k x}{L}\right)$ for $k \in \mathbb{Z}$ with associated eigenvalues

$$\lambda_k^{\text{SH}} = - \left(1 - \frac{4(\pi k)^2}{L^2}\right)^2 \quad \text{for } k \in \mathbb{Z}.$$

For simplicity, we consider $L = 2\pi$: then $\lambda_0^{\text{SH}} = -1$, $\lambda_k^{\text{SH}} = -(1 - k^2)^2$, and $k = \pm 1$ yield elements in $\text{nullspace}(A_{\text{SH}})$. For $k \neq \pm 1$, we have $\lambda_k^{\text{SH}} \leq -1$. Linearizing (2) around the trivial solution $u \equiv 0$, leads to the linear problem

$$\partial_t U = (r_{\text{SH}} \text{Id} + A_{\text{SH}})U = AU, \quad U \in X.$$

Hence, we observe that $u \equiv 0$ is linearly stable for $r_{\text{SH}} < 0$ and that a bifurcation occurs at $r_{\text{SH}} = 0$. For a detailed bifurcation analysis of the SH equation we refer to [15, 19, 23] and references therein. When we consider a stochastic version of (2) below, we focus on the parameter regime $r_{\text{SH}} \in [-r_0, 0)$ for some $r_0 > 0$, since it is our goal to find early-warning signs before the bifurcation occurs.

As a second example, we study the real Ginzburg-Landau (GL) equation [20, 79], which can also be written in the form (1). It is given by

$$\partial_t u = r_{\text{GL}} u + \partial_x^2 u - u^3 = r_{\text{GL}} u + A_{\text{GL}} u - u^3, \quad (3)$$

where $r_{\text{GL}} \in \mathbb{R}$ is a parameter. The Laplacian ∂_x^2 with periodic boundary conditions on $[0, L]$ has eigenfunctions

$$\frac{1}{L} \exp\left(\frac{2\pi}{L} i k x\right) \quad (4)$$

with eigenvalues $\lambda_k^{\text{GL}} = -4k^2\pi^2/L^2$. Note that, as before, the basis (4) is orthonormal in $L^2([0, L])$, and that this general result applies to the linearization of the GL equation. Hence, the analysis yields that $u \equiv 0$ is linearly stable when $r_{\text{GL}} < 0$ and the first eigenvalue crossing occurs when $r_{\text{GL}} = 0$ associated to the critical eigenvalue $\lambda_0^{\text{GL}} = 0$. As in the SH equation, we would like warning signs to predict the bifurcation point from data obtained in the parameter regime $r_{\text{GL}} \in [-r_0, 0)$ for some $r_0 > 0$.

We remark that there is a classical connection between the SH and GL equations: the GL equation can be derived as an amplitude equation of the SH equation [20, 48]. Here, however, we take the view of studying it independently. The view of GL as an amplitude equation, and the relation between warning signs for the two models, will be considered in future work.

2.2 The Stochastic PDE(s)

One efficient approach for obtaining early-warning signs near bifurcation-induced critical transitions is to use stochastic perturbations to measure the effect of critical slowing down before the bifurcation point, for example through variance and autocorrelation. For some univariate time series, using ordinary differential equations (ODEs) to model deterministic dynamics leads quite naturally to SODEs [52]. Following the same paradigm, we search for warning signs for SPDEs that arise by stochastic perturbations of (1). Consider SPDEs of the form

$$\partial_t u = Au + f(u) + \sigma \xi(x, t), \quad (5)$$

where $(x, t) \in \mathcal{I} \times [0, T]$, $u = u(x, t)$, the function F is assumed to be sufficiently smooth map, $\sigma > 0$ controls the noise level and the noise process $\xi(x, t)$ must be specified. Often the noise term is specified through its correlation function

$$\mathbb{E}[\xi(x, t)\xi(y, s)] = C_{\text{tem}}(t, s)C_{\text{spa}}(x, y), \quad (6)$$

where C_{tem} denotes the temporal correlation function and C_{spa} the spatial correlation function. For example, space-time white noise is given by

$$C_{\text{tem}}(t, s) = \delta(t - s) \quad \text{and} \quad C_{\text{spa}}(x, y) = \delta(x - y),$$

where δ denotes the delta-distribution. Although this formulation is quite practical, here the term $\sigma F(u)\xi(x, t)$ is formal but it can be defined rigorously [84] in certain situations; see also [39, 36].

We now describe one way to provide a rigorous interpretation of (5) following the approach in [71, 72]. We fix a probability space $(\Omega, \mathcal{F}, \mathbb{P})$ and let $Q : X \rightarrow X$ be a linear operator on the Hilbert space X with associated Q -Wiener process $W = W(t)$. If $\text{Tr}(Q) < +\infty$ the operator Q is of trace class. If $Q = \text{Id}$ then $\text{Tr}(Q) = +\infty$ and W is a cylindrical Wiener process. We assume that there exists a complete orthonormal set of eigenfunctions $\{q_k\}_{k=-\infty}^{\infty} \subset X$ with associated nonnegative eigenvalues $\{\rho_k\}_{k=-\infty}^{\infty} \subseteq [0, \infty)$ such that

$$Qq_k = \rho_k q_k \quad \text{for } k \in \mathbb{Z}. \quad (7)$$

Let $\beta_k(t)$ denote a sequence of independent standard Brownian motions such that

$$W(t) = \sum_{k=-\infty}^{\infty} \sqrt{\rho_k} \beta_k(t) q_k. \quad (8)$$

We remark that frequently one indexes q_k and β_k by natural numbers only but here the integer labels will be easier notationally. It is often convenient to take $X = L^2(\mathcal{I})$, as already considered above for the deterministic case. We focus on additive noise for (5) and write it in the form

$$du = (Au + f(u)) dt + \sigma B dW_t, \quad u(x, 0) = u_0(x), \quad (9)$$

where $W(t)$ is a Q -Wiener process, f is a sufficiently smooth map, $B : X \rightarrow X$ is a linear operator, $\sigma > 0$ and $u_0 \in X$ is assumed to be deterministic. For our purposes, it will suffice to view (9) as an evolution equation for $u(\cdot, t) =: u(t)$ and formally consider mild solutions [72, Ch.7] given by

$$u(t) = S(t)u_0 + \int_0^t S(t-s)f(u(s)) ds + \sigma \int_0^t S(t-s)B dW(s). \quad (10)$$

For convenience, we denote the stochastic integral in (10) as

$$W_A(t) = \int_0^t S(t-s)B dW(s)$$

and refer to it as the stochastic convolution. One of its most important properties is the expression for the associated covariance operator [72, Thm. 5.2]

$$V(t) := \text{Cov}(W_A(t)) = \int_0^t S(r) B Q B^* S^*(r) \, dr \quad (11)$$

where B^* denotes the adjoint operator of B and similarly $S^*(r)$ denotes the adjoint semigroup of $S(r)$.

We remark that once the operators Q and B are fixed, this determines the correlation structure of the additive noise as defined in (6). Indeed, we have for any $g, h \in X$ and $t, s \geq 0$ that

$$\mathbb{E}[\langle W_{\text{Id}}(t), g \rangle \langle W_{\text{Id}}(s), h \rangle] = \min(t, s) \langle B Q B^* g, h \rangle,$$

which is equivalent to the more detailed formulation

$$\int_{\mathcal{I}} \int_{\mathcal{I}} \mathbb{E}[W_{\text{Id}}(t) W_{\text{Id}}(s)] g(x) h(y) \, dx \, dy = \min(t, s) \int_{\mathcal{I}} Q^{1/2} B^* g(v) Q^{1/2} B^* h(v) \, dv,$$

since Q is self-adjoint. If we consider the basis q_k , then we also find

$$\begin{aligned} Q^{1/2} B^* g &= \sum_{k=-\infty}^{\infty} \langle g, q_k \rangle Q^{1/2} B^* q_k = \sum_{k=-\infty}^{\infty} \langle g, q_k \rangle \sum_{l=-\infty}^{\infty} \sqrt{\rho_l} \langle B^* q_k, q_l \rangle q_l \\ &= \sum_{l,k=-\infty}^{\infty} \sqrt{\rho_l} \int_{\mathcal{I}} g(x) q_k(x) \, dx \underbrace{\int_{\mathcal{I}} q_k(y) (B q_l)(y) \, dy}_{=: b_{kl}} q_l. \end{aligned}$$

and similarly for $Q^{1/2} B^* h$. Therefore, it follows that

$$\begin{aligned} &\int_{\mathcal{I}} Q^{1/2} B^* g(v) Q^{1/2} B^* h(v) \, dv \\ &= \int_{\mathcal{I}} \sum_{k,l=-\infty}^{\infty} b_{kl} \sqrt{\rho_l} \int_{\mathcal{I}} g(x) q_k(x) \, dx \, q_l(v) \sum_{m,n=-\infty}^{\infty} b_{mn} \sqrt{\rho_n} \int_{\mathcal{I}} h(y) q_m(y) \, dy \, q_n(v) \, dv \\ &= \int_{\mathcal{I}} \int_{\mathcal{I}} \sum_{l=-\infty}^{\infty} \rho_l \left(\sum_{k=-\infty}^{\infty} b_{kl} q_k(x) \right) \left(\sum_{m=-\infty}^{\infty} b_{ml} q_m(y) \right) g(x) h(y) \, dx \, dy \\ &= \int_{\mathcal{I}} \int_{\mathcal{I}} \sum_{l=-\infty}^{\infty} \rho_l \sum_{n=-\infty}^{\infty} c_{nl}(x, y) g(x) h(y) \, dx \, dy, \end{aligned}$$

where c_{nl} is computed from the discrete convolution in the usual way

$$c_{nl}(x, y) = \sum_{j=-\infty}^{\infty} b_{jl} b_{(n-j)l} q_j(x) q_{n-j}(y).$$

This gives $C_{\text{spa}}(x, y) = \sum_{l=-\infty}^{\infty} \rho_l \sum_{n=-\infty}^{\infty} c_{nl}(x, y)$, which is colored noise in general. The temporal correlation is white, since differentiating $\min(t, s)$ formally yields a temporal correlation function $C_{\text{tem}}(t - s) = \delta(t - s)$. The relation between the correlation function and a suitable convolution involving B and Q is well-known when $\mathcal{I} = \mathbb{R}^d$ [14, 70].

To conclude our discussion of SPDEs, we briefly review several works pertaining to stochastic perturbations to the SH equation in particular. Additive noise, i.e. when $F(u)$ is constant, is considered in [34, 43] with a comparison to experimental data. Multiplicative noise, i.e. when $F(u)$ depends upon u nontrivially, is studied in [32] with a focus on noise-induced shifts of the bifurcation point. Such bifurcation-shifts are also considered in [45, 46] for additive noise, and in [3] for stochastic variation of the bifurcation parameter. Parameter fluctuations may also induce stochastic resonance effects in the SH equation [82] (for coherence resonance induced by additive noise, see [17]). Pattern formation, pattern selection and convergence to various states in the presence of stochasticity is considered in [30, 41, 83]. The amplitude equations for the stochastic SH equation and related models have also been studied extensively in recent years [1, 8, 9, 11, 12, 66]. However, there seems to be relatively little, if any, work yet that focuses on early-warning signs for the stochastic SH equation.

3 Warning Signs from Linearization

When considering early-warning signs in SODEs perturbed by additive noise, it is illustrative to start with a linearized analysis around a parametrized curve of attracting steady states of the deterministic system. This yields an Ornstein-Uhlenbeck (OU) process that has certain increasing elements in its covariance matrix as a bifurcation point is approached [52]. Of course, the regime very close to the bifurcation is more difficult to study analytically, especially if the parameter drifts slowly in time, e.g. [4, 6]. For SPDEs, our analytical approach focuses only on the regime in which a linearized analysis is expected to be valid. In fact, there are already many results for OU processes of SPDEs that can be used directly to develop the theory of early-warning signs for SPDEs.

3.1 Correlation Function

Consider an SPDE of the form (5) with $F(u) = \text{Id}$ and $f(u) = 0$, i.e. a linear SPDE perturbed by additive noise. We recall a few formal results about the correlation structure of the solution $u(x, t)$ when $\xi(x, t)$ is space-time white noise. For $A = r\text{Id} + \partial_x^2$, $r < 0$, $\mathcal{I} = [0, L]$ and periodic boundary conditions, the solution $u(x, t)$ can be written in terms of a Fourier basis and an associated Green's function [63] as

$$u(x, t) = \int_{\mathcal{I}} G(x, v, t, 0) u_0(v) \, dv + \sigma \int_0^t \int_{\mathcal{I}} G(x, v, t, s) \, dv \, dW(s), \quad (12)$$

where $W(s)$ is a cylindrical Wiener process with covariance $Q = \text{Id}$ and the Green's function G is given by

$$G(x, v, t, s) = \frac{\exp(-2r(t-s))}{2\sqrt{\pi(t-s)}} \sum_{k=-\infty}^{\infty} \exp\left(-\frac{(x-v-kL)^2}{4(t-s)}\right).$$

We define the correlation function of the solution $u(x, t)$ as

$$c(x, y, s, t) := \mathbb{E}[u(x, t)u(y, s)]. \quad (13)$$

In formula (12), we observe that the first term decays rapidly for sufficiently bounded initial conditions u_0 so that the correlation function (13) arises primarily from the stochastic integral. By spatial translation invariance, the correlation function only depends upon the difference $|x - y|$. An asymptotic result obtained in [63, 64] is that

$$\lim_{t \rightarrow \infty} c(u, 0, t, t) = \frac{\epsilon^2}{4\sqrt{|r|}} e^{-|u|\sqrt{|r|}}. \quad (14)$$

Formulas for the correlation function in higher-dimensions (arising from rather involved calculations) exist [68, 63, 64]. The Fourier transform in combination with Bessel potential solutions [31, Sec. 4.3] may also be used to calculate the correlation function for the $\mathcal{I} = \mathbb{R}$ as shown in [39, Sec. 2.3]. However, the formula (14) suffices here to illustrate that we can expect an increasing correlation length as $r \rightarrow 0^-$. This certainly provides some confidence that an SPDE should exhibit early-warning signs before bifurcations.

At this point, the formal and asymptotic calculations of the correlation function for linear PDEs involving the Laplacian and a space-time white-noise driving term are already quite complicated. If a more complex space-time correlation structure is specified via C_{tem} and C_{spa} , or if a different linear operator A is chosen, there may be no closed form expression for (13). Hence, it appears very useful to consider an abstract framework to study generic covariance-related early-warning signs.

3.2 The Covariance Operator

An alternative approach that does not immediately yield explicit formulas is to use the covariance operator from (11). Suppose $F(u) = \text{Id}$ and $f(u) = 0$ so that (9) is a linear SPDE with additive noise and solution given by

$$u(x, t) = S(t)u_0 + \sigma W_A(t).$$

Then, using (8), we can write the solution as the stochastic convolution

$$u(x, t) = S(t)u_0 + \sigma \sum_{k=-\infty}^{\infty} \sqrt{\rho_k} \int_0^t S(t-s) B q_k \, d\beta_k(s), \quad (15)$$

where the detailed definition of the integral is given in [71, Sec. 2.2]. The main result [71, Prop. 2.2] requires, aside from the usual strong continuity assumption on $S(t)$ and linearity for $B : X \rightarrow X$, that the operator $V(t)$ is of trace class $\text{Tr}(V(t)) < +\infty$. Under these assumptions, the series in (15) is convergent in $L^2(\Omega, \mathcal{F}, \mathbb{P}; X)$. Furthermore, $W_A(t)$ is a Gaussian random variable with mean $S(t)u_0$ and covariance operator $V(t)$, that satisfies

$$\mathbb{E}[|W_A(t)|^2] = \text{Tr}(V(t)).$$

We continue to assume that $r < 0$ so that

$$\|S(t)\| \leq Me^{\omega t}$$

for some $M > 0$ and $\omega < 0$. In particular, $\|S(t)u_0\|_X \rightarrow 0$ as $t \rightarrow +\infty$, so we may neglect the first term $S(t)u_0$ if we are only interested in the asymptotic behavior as $t \rightarrow +\infty$; alternatively, we could set $u_0(x) = 0$ for all $x \in \mathcal{I}$. Then $u(x, t) = \sigma W_A(t)$ and there exists a unique invariant Gaussian measure with mean zero and covariance operator $V_\infty := \lim_{t \rightarrow +\infty} V(t)$ [71, Thm. 2.34]. V_∞ is a linear continuous operator that satisfies $\langle V_\infty g, g \rangle \geq 0$ for all $g \in X$ and $V_\infty = V_\infty^*$. Furthermore, V_∞ satisfies a Lyapunov equation [71, Lem. 2.45] given by

$$\langle V_\infty g, A^* h \rangle + \langle A^* g, V_\infty h \rangle = -\sigma^2 \langle BQB^* g, h \rangle, \quad (16)$$

which is a generalization of the classical Lyapunov equation associated with linear SODEs used to determine scaling laws for warning signs [52]. In fact, a suitable analog of (16) even holds for transition semigroups in more general Banach spaces [35, Sec. 4]. For SODEs, solving (16) requires solving a matrix-valued equation, which can not only be solved analytically for certain cases but can also be efficiently solved numerically for general nonlinear parametrized stochastic systems [51].

Solving (16) is more problematic for infinite-dimensional operators. A natural first attempt is to compute the operator using a suitable basis of X . However, there are two natural bases to consider. For one, we can use the eigenbasis $\{q_k\}_{k=-\infty}^\infty$ of Q given in (7). Alternatively, we can use

$$Aa_k = ra_k + A_{(\cdot)}a_k = (r + \lambda_k^{(\cdot)})a_k, \quad a_k \in X, \quad k \in \mathbb{Z}$$

so that a_k are eigenfunctions for A (respectively $A_{(\cdot)}$). In either case, there are now several straightforward and instructive calculations we can carry out to understand potential early-warning signs related to V_∞ .

First, we consider the case in which $B = \text{Id}$ and $a_k = q_k$ for all $k \in \mathbb{Z}$ is an orthonormal basis of X ; the operator A has eigenvalues $\lambda_k = r + \lambda_k^{(\cdot)}$ and the operator Q has eigenvalues ρ_k in this basis. The operator V_∞ is completely determined if we can compute the coefficients $\langle V_\infty a_k, a_j \rangle$ for all $k, j \in \mathbb{Z}$. From (16), we find

$$\begin{aligned} 0 &= \langle V_\infty a_k, A^* a_j \rangle + \langle A^* a_k, V_\infty a_j \rangle + \sigma^2 \langle Q a_k, a_j \rangle \\ &= \langle V_\infty a_k, \overline{\lambda_j} a_j \rangle + \langle \overline{\lambda_k} a_k, V_\infty a_j \rangle + \sigma^2 \langle \rho_k a_k, a_j \rangle \\ &= \lambda_j \langle V_\infty a_k, a_j \rangle + \overline{\lambda_k} \langle V_\infty a_k, a_j \rangle + \sigma^2 \rho_k \langle a_k, a_j \rangle. \end{aligned}$$

Using orthonormality of the basis it follows that

$$\langle V_\infty a_k, a_j \rangle = \begin{cases} -\sigma^2 \frac{\rho_k}{\lambda_k + \overline{\lambda_k}}, & \text{if } k = j, \\ 0, & \text{if } k \neq j \text{ (and } \lambda_j \neq -\overline{\lambda_k}). \end{cases}$$

We note that $\lambda_j \neq -\overline{\lambda_k}$ as long as we have $\text{Re}(\lambda_k) < 0$ for all $k \in \mathbb{Z}$. Therefore, the operator V_∞ is diagonal and the important coefficients (for $r < 0$) are

$$\langle V_\infty a_k, a_k \rangle = -\sigma^2 \frac{\rho_k}{\lambda_k + \overline{\lambda_k}} = -\sigma^2 \frac{\rho_k}{2r + \lambda_k^{(\cdot)} + \overline{\lambda_k^{(\cdot)}}} = -\sigma^2 \frac{\rho_k}{2 \left(r + \text{Re} \left(\lambda_k^{(\cdot)} \right) \right)} \geq 0,$$

where the last inequality follows from $\rho_k \geq 0$ and $r + \text{Re}(\lambda_k^{(\cdot)}) < 0$ when $r < 0$. Now we can consider particular eigenvalues $\lambda_k^{(\cdot)}$ for the SH and GL linearized operators. For example, in the SH equation we have $\lambda_{\pm 1}^{\text{SH}} = 0$ as critical eigenvalues. Hence, we find the divergent coefficients

$$\lim_{r \rightarrow 0^-} \langle V_\infty a_{\pm 1}, a_{\pm 1} \rangle = \lim_{r \rightarrow 0^-} -\sigma^2 \frac{\rho_{\pm 1}}{2r} = +\infty,$$

for fixed $2\rho_{\pm 1} > 0$. This represents an $\mathcal{O}(1/r)$ variance scaling law as $r \rightarrow 0^-$ ($\sigma > 0$ is fixed) for the linearized system, which resembles the variance scaling laws associated with finite-dimensional bifurcation points (e.g. [52, Thm 5.1] or [4]). The same scaling law applies to the GL equation with critical eigenvalue $\lambda_0^{\text{GL}} = 0$. We remark that if $\rho_{\pm 1} = 0$, then no such scaling law can be expected. Of course, spatio-temporal noise with $\rho_{\pm 1} = 0$ is a highly degenerate scenario, and is not expected to occur often in practice.

Next, we consider the more general case with a linear operator B and in which the orthonormal eigenbases of A and Q do not coincide. The Lyapunov equation (16) gives that

$$0 = \lambda_j \langle V_\infty a_k, a_j \rangle + \overline{\lambda_k} \langle V_\infty a_k, a_j \rangle + \sigma^2 \langle BQB^* a_k, a_j \rangle.$$

This implies

$$\langle V_\infty a_k, a_j \rangle = -\sigma^2 \frac{\langle BQB^* a_k, a_j \rangle}{\lambda_j + \overline{\lambda_k}} = -\sigma^2 \frac{\langle BQB^* a_k, a_j \rangle}{2r + \lambda_j^{(\cdot)} + \overline{\lambda_k^{(\cdot)}}}.$$

If the eigenvalues $\lambda^{(\cdot)}$ are real, as they are for the SH and GL equations considered here, it follows that

$$\langle V_\infty a_k, a_j \rangle = -\sigma^2 \frac{\langle BQB^* a_k, a_j \rangle}{2r + \lambda_j^{(\cdot)} + \lambda_k^{(\cdot)}}. \quad (17)$$

Hence, V_∞ is generically non-diagonal, i.e.

$$\langle BQB^* a_k, a_j \rangle \neq 0 \quad \text{for all } k, j \in \mathbb{Z}.$$

We have already computed the eigenvalues for the SH and GL equations. For example, for the SH equation with $L = 2\pi$, we have

$$2r + \lambda_j^{\text{SH}} + \lambda_k^{\text{SH}} = 2r - (1 - j^2)^2 - (1 - k^2)^2.$$

Hence if $\langle BQB^*a_k, a_j \rangle \neq 0$ for $k, j = \pm 1$ then a leading-order scaling law for $\langle V_\infty a_k, a_j \rangle$ of order $\mathcal{O}(1/r)$ as $r \rightarrow 0^-$ is observed for the four coefficient pairs

$$(k, j) \in \{(1, 1), (1, -1), (-1, 1), (-1, -1)\}.$$

In principle, these results can be worked out not only for the SH and GL linearized operators but for any SPDE of the form (9). As with SODEs, this should be done by linearizing about a steady state of the deterministic system, operating in a regime below the first destabilizing bifurcation point and using the Lyapunov equation to compute the scaling law for the associated covariance operator V_∞ . We emphasize that this approach does not cover the truly nonlinear regime very close to the bifurcation point, and that a specialized analysis will be necessary here; we discuss scaling laws in this regime further in Section 5.

As another example, we consider the GL equation with $L = 2\pi$. The eigenvalues are then $\lambda_k^{\text{GL}} = -k^2$. Therefore, we find

$$\langle V_\infty a_k, a_j \rangle = -\sigma^2 \frac{\langle BQB^*a_k, a_j \rangle}{2r - (k^2 + j^2)}. \quad (18)$$

and we again observe the $\mathcal{O}(1/r)$ -scaling law for the critical mode when $k = j = 0$. If we increase the domain size and consider $L = 2\pi l$ for some $l \in \mathbb{N}$ and $l \gg 1$, then (18) becomes

$$\langle V_\infty a_k, a_j \rangle = -\sigma^2 \frac{\langle BQB^*a_k, a_j \rangle}{2r - (k^2 + j^2)/l^2}. \quad (19)$$

since the eigenvalues of the Laplacian become $\lambda_k^{\text{GL}} = -k^2/l^2$. Thus, the $\mathcal{O}(1/r)$ scaling law begins to appear in all modes if we take the formal limit $l \rightarrow \infty$ before considering $r \rightarrow 0^-$.

This linearized analysis is a first step towards identifying early-warning signs in SPDEs, and a more complete analysis should also include contributions from nonlinearities, especially when r is very close to the bifurcation point at $r = 0$. This may be accomplished using the amplitude equation derived from the full nonlinear SPDE as shown in [9]; see also [10]. We do not pursue this approach in this paper, instead leaving it for future work.

4 Spatio-Temporal Early-Warning Signs

Rather than pursuing the abstract theory further, we proceed by examining several generic early-warning signs that have been suggested for spatio-temporal processes; see also the references in Section 2.2.

Measures of one-point temporal variance and correlation for spatio-temporal processes, which track temporal statistics at one spatial point, are natural extensions of the generic early-warning signs developed for univariate time series [73]. Previous studies have computed these measures in moving windows for various two-dimensional (2D) processes generated by simulations in which a parameter drifts slowly in time, finding that signals of impending transitions are sometimes obscured by past measurements in the moving window [29, 27]. For a process generated by a pattern-forming vegetation model, however, autocorrelation at lag 1 is found to increase monotonically approaching a Turing bifurcation [25].

More robust signals of critical transitions in spatio-temporal processes are expected to lie in explicitly spatial measures. Such measures computed at points in time, in contrast with temporal measures computed in a moving window, reflect the instantaneous (rather than residual) state of a system [38]. Spatial variance, skewness, correlation length, and patchiness have previously been shown to increase before a sudden transition for various 2D processes [38, 29, 27, 25].

In Section 5, we analyze solutions $u = u(x, t)$ of the SH and GL SPDEs. To emphasize dependence upon the parameter r , we henceforth write $u = u(x, t; r)$. Previously, we showed in Section 3.2 that for fixed $r < 0$, sufficiently far from $r = 0$ and with sufficiently small initial conditions, the linear approximation leads to a stochastic scaling law of the covariance operator. In this regime, the long-time dynamics ($t \rightarrow \infty$) of the process $u(x, t; r)$ is well-approximated by an invariant Gaussian measure with mean zero and covariance operator $V_\infty(t; r)$.

One natural measure to consider is the variance of $u(x, t; r)$, which we compute by averaging spatial variance over time:

$$V(r) = \frac{1}{NM} \sum_{n,j=1}^{N,M} \left(u(x_j, t_n; r) - \frac{1}{N} \sum_{j=1}^N u(x_j, t_n; r) \right)^2.$$

We note that $V(r)$ is approximately equal to the temporal variance averaged over space,

$$V(r) \approx \frac{1}{NM} \sum_{n,j=1}^{N,M} \left(u(x_j, t_n; r) - \frac{1}{M} \sum_{n=1}^M u(x_j, t_n; r) \right)^2,$$

since $\frac{1}{N} \sum_{j=1}^N u(x_j, t; r) \approx \frac{1}{M} \sum_{n=1}^M u(x, t_n; r) \approx 0$ as long as M, N are sufficiently large. This example suggests how temporal and spatial variance can be related as early-warning signs in general.

In analogy to the univariate early-warning sign, we also compute the autocorrelation as a function of time lag l , averaged over space:

$$R_l(r) = \frac{1}{N} \sum_{j=1}^N \frac{\sum_{n=1}^{M-l} (u(x_j, t_n; r) - \bar{u}(x_j; r)) (u(x_j, t_{n+l}; r) - \bar{u}(x_j; r))}{\sum_{n=1}^M (u(x_j, t_n; r) - \bar{u}(x_j; r))^2},$$

where $\bar{u}(x; r) = \frac{1}{M} \sum_{n=1}^M u(x, t_n; r)$. Another measure not typically considered as an early-warning sign is the supremum of the process over all space and time:

$$\mathcal{S}(r) = \sup_{t \in [0, T]} \sup_{x \in \mathcal{I}} |u(x, t; r)|.$$

This measure generally depends on the end time, T , since large deviations occur as rare events. We may expect (as with white noise) that $\mathcal{S}(r) \rightarrow \infty$ as $T \rightarrow \infty$, but the rate at which certain maxima or minima of the stochastic process diverge as $T \rightarrow \infty$ may be different for different values of r .

Additionally, it is of particular interest for our analysis of pattern-forming SPDEs to consider spatial statistics in Fourier space. In order to compare numerical results with theoretical predictions as in Section 3.2, we compute

$$V_k(r) = \frac{1}{M} \sum_{n=1}^M (|\hat{u}(k, t_n; r)| - \bar{u}(k; r))^2,$$

where $\hat{u}(k, t) = \frac{1}{L} \int_{\mathcal{I}} u(x, t) \exp(-2\pi i k x / L) dx$ and $\bar{u}(k; r) = \frac{1}{M} \sum_{n=1}^M |\hat{u}(k, t_n; r)|$.

5 Numerical Results

Several previous studies of early-warning signs in spatial systems consider a parameter that drifts slowly in time [38, 29, 27, 25]. Here, we essentially consider the limit as the parameter drift rate vanishes by simulating the SPDE (5) using a series of fixed parameter values. We do this in order to relate the numerical results directly to the analytical results described in Section 3. Furthermore, this approach guarantees well-defined stationary early-warning measures as described in Section 4; the analysis of a slowly-drifting parameter is postponed for future work.

To verify the scaling laws derived in Section 3.2, we numerically simulated the GL and SH SPDEs in the form of (5), with $F(u) = 1$ and $\sigma = 0.01$. We begin with $\xi(x, t)$ as space-time white noise. Simulations were run for values of $r \in [-1, -0.01]$ on domains of size $L = 2\pi$ and $L = 16\pi$ with periodic boundary conditions. A spatial finite-difference method was used to discretize the SPDEs. The resulting SODEs were solved by an implicit Euler-Maruyama method. For a more detailed description of the numerical method we refer to Appendix A.2.

One set of predictions obtained by linearization in Section 3.2 pertains to the $\mathcal{O}(1/r)$ scaling of variance in critical eigenfunction modes of the GL and SH operators for the domain size $L = 2\pi$. Indeed, such scaling is observed in the critical Fourier modes ($k = 0$ for GL and $k = 1$ for SH) when V_k is computed for one set of numerical simulations. Figure 1 plots $\log_{10}(-r)$ against $\log_{10}(V_k)$, with a guide line $\sim \log_{10}(-1/r)$. When r is sufficiently far from $r = 0$ (i.e. when the linearization is a good approximation), the critical Fourier modes appear to follow the predicted scaling. For comparison, the V_k

measures for adjacent modes are also plotted and are observed to scale much more slowly than $\mathcal{O}(1/r)$.

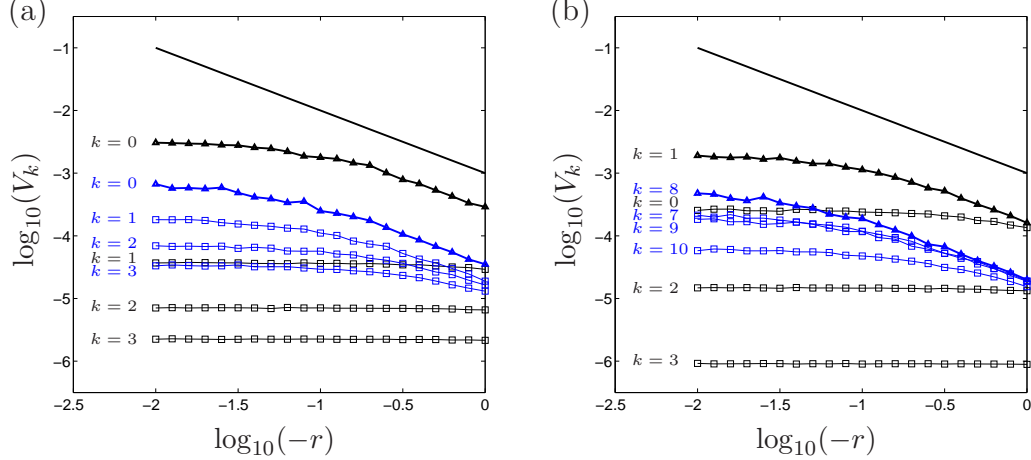


Figure 1: Log-log plot of variances of critical (\triangle) and near-critical (\square) Fourier modes in solutions of the (a) GL and (b) SH SPDEs, depending on the parameter $r \in [-1, -0.01]$; solutions are computed using domain sizes $L = 2\pi$ (black) and $L = 16\pi$ (blue); a guide line $\sim -1/r$ is plotted in solid black. Here we have chosen $\xi(x, t)$ to be space-time white noise, $F(u) = 1$ and $\sigma = 0.01$. SPDEs were numerically as described in Appendix A.2).

Another set of predictions from Section 3.2 describes the scaling of variance in non-critical modes when $L \gg 2\pi$. Equation (19) shows that an $\mathcal{O}(1/r)$ scaling should appear in all modes for the GL operator as $L \rightarrow \infty$, and it can similarly be shown that an approximate $\mathcal{O}(1/r)$ scaling should appear in near critical modes for the SH operator under the same limit. This, too, is observed for a set of numerical simulations with $L = 16\pi$. Figure 1 shows also the log-variance of critical ($k = 0$ for GL and $k = 8$ for SH) and near-critical Fourier modes in the larger domain for the GL and SH operators, and the $\mathcal{O}(1/r)$ scaling is observed for the closest-to-critical modes.

We notice in Figure 1 that a $\mathcal{O}(1/r)$ scaling only applies to a parameter regime sufficiently far from $r = 0$. We interpret this as the regime in which linearization is valid. For both SH and GL equations, it can be shown that a regime of weak nonlinearity occurs where $r = \mathcal{O}(|A|^2)$ [23, 22], where A is the critical Fourier mode amplitude. Thus, we expect that as the noise level σ decreases, $|A|$ decreases as well and the linear results should hold for a larger parameter regime. We confirm this numerically in Figure 2 using simulations of the GL and SH equations with $\sigma = 0.01$ and $\sigma = 0.001$. Critical mode variances are observed to follow a $\mathcal{O}(1/r)$ scaling for a larger parameter regime when the smaller noise level, $\sigma = 0.001$, is used.

To explore the relationship between the measures described in Section 4 and the factors of domain size, noise type, and noise correlation length, we numerically sim-

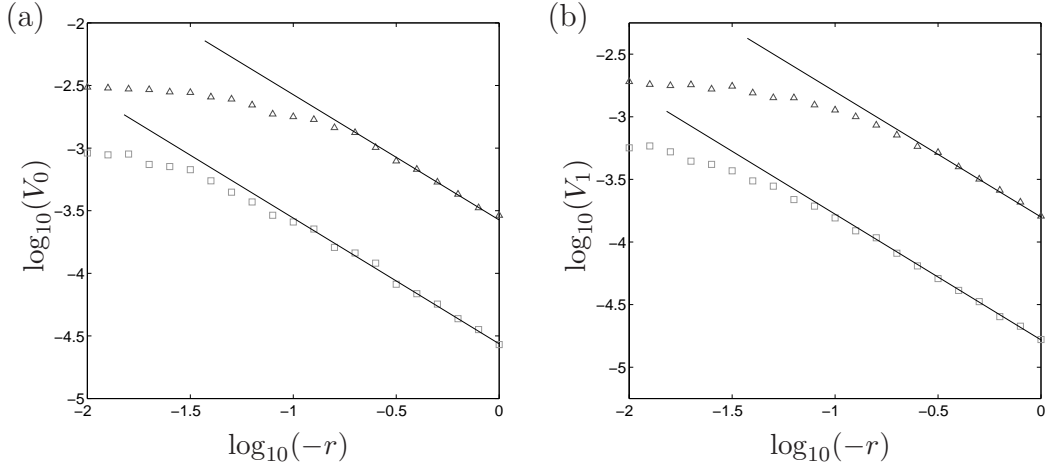


Figure 2: Log-log plot of variances of critical Fourier modes in solutions of the (a) GL and (b) SH SPDEs, depending on the parameter $r \in [-1, -0.01]$; solutions are computed using noise levels $\sigma = 0.01$ (\triangle) and $\sigma = 0.001$ (\square); guide lines $\sim -1/r$ is plotted in solid black. We take $L = 2\pi$, $\xi(x, t)$ to be space-time white noise and $F(u) = 1$.

ulated the SH SPDE for values of $r \in [-1, 0]$. For some of these simulations, alternative domain sizes of $L = 2\pi$ and $L = 16\pi$ are considered. For other simulations, $\xi(x, t)$ is generated as either space-time white noise or noise that is colored in space, i.e. $\mathbb{E}[\xi(x, t)\xi(y, s)] = C_{\text{spa}}(x, y)\delta(t - s)$. The form $C_{\text{spa}}(x, y) = \exp((x - y)^2/\eta)$ was chosen, with $\eta = 1/32$ representing a short correlation length and $\eta = 1/8$ representing an intermediate correlation length for domain size $L = 2\pi$. Details about the generation of space-colored noise are described in Appendix A.1. Numerical parameter values and simulation details are otherwise as previously described.

Figure 3 compares the effect of white noise and spatially-colored noise on the scaling of R_1 , V , and \mathcal{S} with r . The domain size $L = 2\pi$ and the noise correlation function $C_{\text{spa}}(x, y) = \exp(32(x - y)^2)$ were used. For both types of noise, all three measures appear to scale with r in a similar way. We observe a clear monotonic increase in lag-1 temporal autocorrelation as $r \rightarrow 0^-$. We also see a near $\mathcal{O}(1/r)$ scaling of the spatial variance when r is sufficiently far from $r = 0$. This reflects the dominant effect of critical mode variance on overall spatial variance (from Figure 1, we observe the variance of non-critical modes is negligible for space-time white noise). Suprema clearly increase as $r \rightarrow 0^-$, as well. The magnitude of variation, as expressed by V and \mathcal{S} , is greater for spatially colored noise, which we conjecture is related to the distribution of energy in the power spectrum of the noise. The energy of space-time white noise is distributed evenly across all non-zero Fourier modes, while energy is concentrated around the SH critical mode ($k = 1$) for noise with the spatial correlation function we consider here.

A similar comparison for two different colored noise correlation lengths is shown in Figure 4. Again, the domain size $L = 2\pi$ was used, and the noise correlation functions

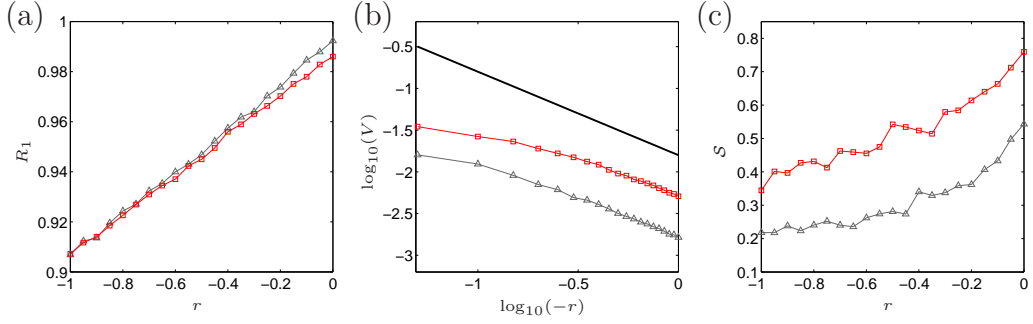


Figure 3: Dependence of spatial and temporal statistics in solutions of the SH SPDE on the parameter $r \in [-1, 0]$; solutions are computed using space-time white noise (\triangle) and spatially colored noise (\square); plots show (a) autocorrelation at time-lag 1, (b) log-log of spatial variance, and (c) supremum of solution over all space and time. We take $L = 2\pi$, $F(u) = 1$, $\sigma = 0.01$, and $C_{\text{spa}}(x, y) = \exp(32(x - y)^2)$ for the colored noise. SPDE was numerically as described in Appendix A.2 and spatially colored noise was generated approximately in Fourier space as discussed in Appendix A.1.

$C_{\text{spa}}(x, y) = \exp(32(x - y)^2)$ (short correlation length) and $C_{\text{spa}}(x, y) = \exp(8(x - y)^2)$ (intermediate correlation length) were considered. For both correlation lengths, all three measures once again appear to scale with r in a similar way. Additionally, we observe that the magnitude of variation is greater for the intermediate correlation length simulations. As before, we conjecture that the reason for this can be found in the noise power spectrum. The intermediate correlation noise has more energy in the critical SH Fourier mode than the short correlation noise in this case.

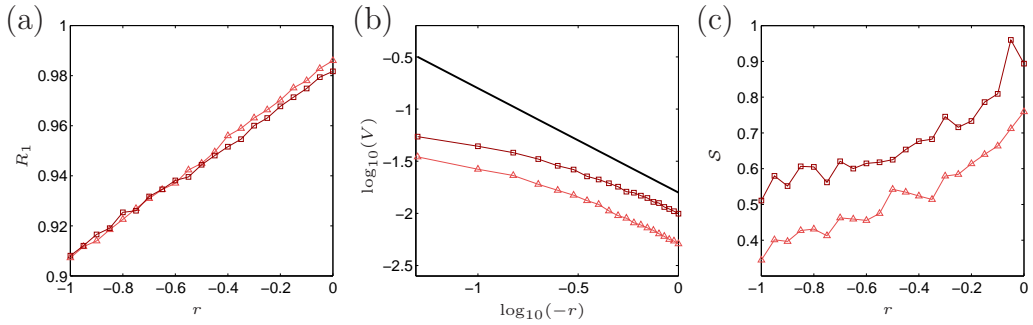


Figure 4: Dependence of spatial and temporal statistics in solutions of the SH SPDE on the parameter $r \in [-1, 0]$; solutions are computed using spatially colored noise with $C_{\text{spa}}(x, y) = \exp(32(x - y)^2)$ (\triangle , short correlation length) and $C_{\text{spa}}(x, y) = \exp(8(x - y)^2)$ (\square , intermediate correlation length); plots show (a) autocorrelation at time-lag 1, (b) log-log of spatial variance, and (c) supremum of solution over all space and time. We take $L = 2\pi$, $F(u) = 1$ and $\sigma = 0.01$.

Finally, Figure 5 shows the effect of domain size on R_1 , V , and \mathcal{S} . Space-time white noise was used for simulations with domain sizes $L = 2\pi$ and $L = 16\pi$. Here,

we observe that domain size has an effect on the autocorrelation signal. Specifically, R_1 for $L = 16\pi$ is less than R_1 for $L = 2\pi$ for all values of $r \in [-1, 0]$. Also, we see that the larger domain size loses the overall $\mathcal{O}(1/r)$ scaling in spatial variance, instead growing more slowly as $r \rightarrow 0^-$. This could have been anticipated from the observed scaling of non-critical modes in Figure 1. We note that suprema appear to scale in the same way for both domain sizes, which suggests a domain size invariant early-warning sign.

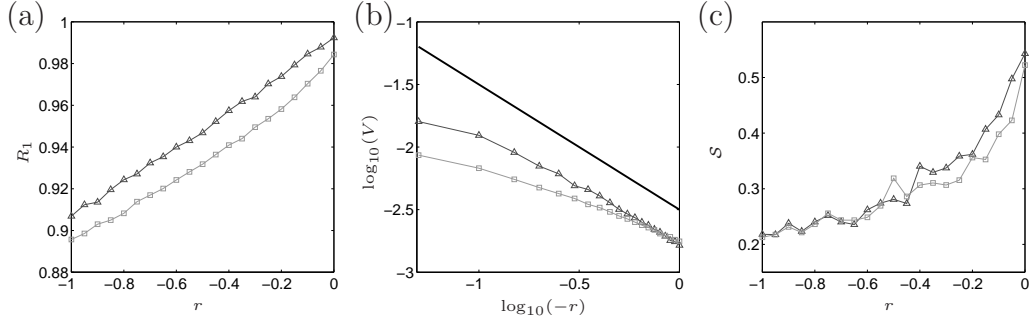


Figure 5: Dependence of spatial and temporal statistics in solutions of the SH SPDE on the parameter $r \in [-1, 0]$; solutions are computed using domain sizes $L = 2\pi$ (\triangle) and $L = 16\pi$ (\square); plots show (a) autocorrelation at time-lag 1, (b) log-log of spatial variance, and (c) supremum of solution over all space and time. We take $\xi(x, t)$ to be space-time white noise, $F(u) = 1$ and $\sigma = 0.01$.

6 Conclusions & Outlook

In this paper, we have started to develop elements of a mathematical theory for early-warning signs in pattern-forming SPDEs, specifically in the homogeneous regime before a Turing bifurcation. In particular, we gave an analytical treatment of the scaling laws for covariance operators of the linearized SPDE problem. This analysis included the linearized GL and SH equations, which we investigated numerically in the second part of this work. In the numerical simulations, we focused on the influence of distance to bifurcation, noise strength, noise color and domain size.

Although we believe that our work provides a basis for the study of early-warning signs in SPDEs, many open problems remain. We have attempted to collect several references from different fields as additional starting points for future research. There are many natural mathematical problems that seem to be of particular interest in spatial early-warning sign applications. For example, given a particular pattern-forming system, can we give precise estimates for different regime sizes and early-warning sign scaling laws in these regimes for the covariance operators (and other statistical measures) of the linearized problem in comparison to the full nonlinear problem? What role do amplitude equations for SPDEs play in this context? How can we classify which

models display warning signs for spatio-temporal patterns? From these questions, it is clear that there are many mathematical challenges that remain to be addressed in order to quantify the the dynamics of stochastic systems operating near instability.

Acknowledgements: KG thanks Mary Silber for useful conversations throughout the duration of this project, and gratefully acknowledges support from the NSF Math and Climate Research Network (DMS-0940262). CK would like to thank the Austrian Academy of Sciences (ÖAW) for support via an APART fellowship. CK acknowledges the European Commission (EC/REA) for support by a Marie-Curie International Reintegration Grant. CK would like to thank Dirk Blömker for inspiring discussion at the workshop “Infinite-Dimensional Stochastic Systems: Theory and Applications” (Wittenberg, January 2014).

A Numerical Methods

A.1 Generation of Colored Noise in Space

The following procedure for generating a noise field $\xi(x, t)$ that is colored in space and white in time is described in [33]. For $\xi(x, t)$ with $x \in (-\infty, \infty)$, it can be shown that if

$$\mathbb{E}[\xi(x, t)\xi(y, s)] = C_{\text{spa}}(x, y)\delta(t - s).$$

and the Fourier transform of $C_{\text{spa}}(x, 0)$ is finite, then

$$\mathbb{E}[\hat{\xi}(k, t)\hat{\xi}(l, s)] = \hat{C}_{\text{spa}}(k)\delta(k + l)\delta(t - s),$$

where hats denote a function transformed to Fourier k -space:

$$\hat{f}(k) = \int_{-\infty}^{\infty} f(x)e^{-ikx}dx.$$

This decoupling of modes in Fourier space can be exploited to construct $\hat{\xi}(k, t)$:

$$\hat{\xi}(k, t) = \sqrt{\hat{C}_{\text{spa}}(k)}\alpha(k, t), \tag{20}$$

where $\alpha(k, t)$ are random variables that are *anticorrelated* in space, drawn from the normal distribution with mean 0 and $\mathbb{E}[\alpha(k, t)\alpha(l, s)] = \delta(k + l)\delta(t - s)$. Generation of $\alpha(k, t)$ is described in Appendix B of [33]. From here, (20) can be transformed back into real space to obtain $\xi(x, t)$. The practical implementation of this approach in MATLAB is performed approximately for $x \in \mathcal{I}$ using the Fast Fourier Transform (FFT):

```
x=linspace(0, L, N+1); x = x(1:N); %spatial domain
Cspa=exp(-(x-L/2).^2)); %example spatial correlation function
```

```

Ck=fft(Cspa); %Fast Fourier transform of the correlation function

%generate anticorrelated noise field in Fourier space
randNums=randn(1,N);
alphak=sqrt(N)*[randNums(1), sqrt(1/2)*(randNums(2:N/2)+...
    1i*randNums(N/2+1:end-1)), randNums(N),...
    sqrt(1/2)*(fliplr(randNums(2:N/2)-1i*randNums(N/2+1:end-1)))];

xik=alphak.*sqrt(Ck);
xi=ifft(xik); %invert Fourier transform

```

A.2 Finite difference solution of SPDE

A finite difference method in space is used to discretize the SPDE in space to obtain SODEs as described below. Then an implicit Euler-Maruyama scheme is used to solve (5) with $F(u) = 1$. The SODE scheme is described in [49, 42]. Space and time are discretized as $(x_1, x_2, \dots, x_N) = (0, \Delta x, \dots, L - \Delta x)$ and $(t_1, t_2, \dots, t_M) = (0, \Delta t, \dots, T)$, and the discrete solution is denoted $u(x_j, t_n) = u_j^n$. The simulations generated for this paper used numerical parameter values $\Delta x = 0.1$, $\Delta t = 2^{-4}$, $T = 4000$, and tolerance = 0.01. Initial conditions were taken to be uniformly random in space and were drawn from the interval $[-0.1, 0.1]$. The spatial derivatives of (5) are discretized using central differencing operators, i.e.

$$\begin{aligned}\partial_x^2 u_j &\approx (u_{j+1} - 2u_j + u_{j-1})/\Delta x^2 \\ \partial_x^4 u_j &\approx (u_{j+2} - 4u_{j+1} + 6u_j - 4u_{j-1} + u_{j-2})/\Delta x^4.\end{aligned}$$

This discretization results in a system of coupled SODEs,

$$du_j = f_j(\mathbf{u}) dt + \sigma dW_j(t), \quad (21)$$

where $\mathbf{u} = (u_1, u_2, \dots, u_N)$. For instance, when f is defined as in (2), f_j is

$$\begin{aligned}f_j(\mathbf{u}) &= (r - 1)u_j - 2(u_{j+1} - 2u_j + u_{j-1})/\Delta x^2 \\ &\quad - (u_{j+2} - 4u_{j+1} + 6u_j - 4u_{j-1} + u_{j-2})/\Delta x^4 - u_j^3.\end{aligned}$$

To satisfy periodic boundary conditions, $u_0 = u_N$, and so on. The solution of (21) at t_{n+1} is implicitly defined by the update equation

$$u_j^{n+1} = u_j^n + \Delta t f_j(\mathbf{u}^{n+1}) + \sigma dW_j^n. \quad (22)$$

Newton's method is used to iteratively solve (22). Explicitly, (22) is written

$$G_j(\mathbf{u}^{n+1}) = u_j^{n+1} - \Delta t f_j(\mathbf{u}^{n+1}) - u_j^n - \sigma dW_j^n = 0.$$

Then the Newton iteration formula (on the index $i = 1, 2, \dots$) for \mathbf{u}^{n+1} is given by

$$\mathbf{u}_{i+1}^{n+1} = \mathbf{u}_i^{n+1} - (DG(\mathbf{u}_i^{n+1}))^{-1} G(\mathbf{u}_i^{n+1}),$$

where $DG(\mathbf{u}_i^{n+1})$ is the Jacobian matrix of $G = (G_1, G_2, \dots, G_N)$ with respect to \mathbf{u} , evaluated at \mathbf{u}_i^{n+1} , and $\mathbf{u}_1^{n+1} = \mathbf{u}^n$. The iteration terminates when $\|u_{i+1}^{n+1} - u_i^{n+1}\|_2$ is less than a prescribed tolerance value.

References

- [1] G. Agez, M.G. Clerc, E. Louvergneaux, and R.G. Rojas. Bifurcations of emerging patterns in the presence of additive noise. *Phys. Rev. E*, 87(4):042919, 2013.
- [2] P. Ashwin, S. Wieczorek, R. Vitolo, and P. Cox. Tipping points in open systems: bifurcation, noise-induced and rate-dependent examples in the climate system. *Phil. Trans. R. Soc. A*, 370:1166–1184, 2012.
- [3] A. Becker and L. Kramer. Linear stability analysis for bifurcations in spatially extended systems with fluctuating control parameter. *Phys. Rev. Lett.*, 73(7):955–958, 1994.
- [4] N. Berglund and B. Gentz. Pathwise description of dynamic pitchfork bifurcations with additive noise. *Probab. Theory Related Fields*, 3:341–388, 2002.
- [5] N. Berglund and B. Gentz. *Noise-Induced Phenomena in Slow-Fast Dynamical Systems*. Springer, 2006.
- [6] N. Berglund, B. Gentz, and C. Kuehn. Hunting French ducks in a noisy environment. *J. Differential Equat.*, 252(9):4786–4841, 2012.
- [7] J. Berwald and M. Gidea. Critical transitions in a model of a genetic regulatory system. *arXiv:1309.7919*, pages 1–19, 2013.
- [8] D. Blömker. Amplitude equations for locally cubic nonautonomous nonlinearities. *SIAM J. Appl. Dyn. Syst.*, 2(3):464–486, 2003.
- [9] D. Blömker. *Amplitude Equations for Stochastic Partial Differential Equations*. World Scientific, 2007.
- [10] D. Blömker and M. Hairer. Multiscale expansion of invariant measures for SPDEs. *Comm. Math. Phys.*, 251(3):515–555, 2004.
- [11] D. Blömker, M. Hairer, and G.A. Pavliotis. Modulation equation for SPDEs on large domains. *Comm. Math. Phys.*, 258:479–512, 2005.
- [12] D. Blömker and W.W. Mohammed. Amplitude equations for SPDEs with cubic nonlinearities. *Stochastics*, 85(2):181–215, 2013.
- [13] C. Boettinger and A. Hastings. Quantifying limits to detection of early warning for critical transitions. *J. R. Soc. Interface*, 9(75):2527–2539, 2012.

- [14] Z. Brzezniak and S. Peszat. Space-time continuous solutions to SPDEs driven by a homogeneous Wiener process. *Studia Math.*, 137:261–299, 1999.
- [15] J. Burke and E. Knobloch. Localized states in the generalized Swift-Hohenberg equation. *Phys. Rev. E*, 73:056211, 2006.
- [16] S.R. Carpenter and W.A. Brock. Rising variance: a leading indicator of ecological transition. *Ecology Letters*, 9:311–318, 2006.
- [17] O. Carrillo, M.A. Santos, J. Garcia-Ojalvo, and J.M. Sancho. Spatial coherence resonance near pattern-forming instabilities. *Europhys. Lett.*, 65(4):452, 2004.
- [18] A.A. Cimatoribus, S.S. Drijfhout, V. Livina, and G. van der Schrier. Dansgaard-Oeschger events: tipping points in the climate system. *Climate of the Past Discussion*, 8(5):4269–4294, 2012.
- [19] P. Collet and J.P. Eckmann. *Instabilities and Fronts in Extended Systems*. Princeton University Press, 1990.
- [20] P. Collet and J.P. Eckmann. The time dependent amplitude equation for the Swift-Hohenberg problem. *Comm. Math. Phys.*, 132(1):139–153, 1990.
- [21] E. Cotilla-Sanchez, P. Hines, and C.M. Danforth. Predicting critical transitions from time series synchrophasor data. *IEEE Trans. Smart Grid*, 3(4):1832–1840, 2012.
- [22] M. Cross and H. Greenside, editors. *Pattern Formation and Dynamics in Nonequilibrium Systems*. CUP, 2009.
- [23] M.C. Cross and P.C. Hohenberg. Pattern formation outside of equilibrium. *Rev. Mod. Phys.*, 65(3):851–1112, 1993.
- [24] V. Dakos, S.R. Carpenter, W.A. Brock, A.M. Ellison, V. Guttal, A.R. Ives, S. Kéfi, V. Livina, D.A. Seekell, E.H. van Nes, and M. Scheffer. Methods for detecting early warnings of critical transitions in time series illustrated using simulated ecological data. *PLoS One*, 7(7):e41010, 2012.
- [25] V. Dakos, S. Kéfi, M. Rietkerk, E.H. van Nes, and M. Scheffer. Slowing down in spatially patterned systems at the brink of collapse. *Am. Nat.*, 177(6):153–166, 2011.
- [26] V. Dakos, M. Scheffer, E.H. van Nes, V. Brovkin, V. Petoukhov, and H. Held. Slowing down as an early warning signal for abrupt climate change. *Proc. Natl. Acad. Sci. USA*, 105(38):14308–14312, 2008.
- [27] V. Dakos, E.H. van Nes, R. Donangelo, H. Fort, and M. Scheffer. Spatial correlation as leading indicator of catastrophic shifts. *Theor. Ecol.*, 3(3):163–174, 2009.

- [28] P.D. Ditlevsen and S.J. Johnsen. Tipping points: early warning and wishful thinking. *Geophys. Res. Lett.*, 37:19703, 2010.
- [29] R. Donangelo, H. Fort, V. Dakos, M. Scheffer, and E.H. Van Nes. Early warnings for catastrophic shifts in ecosystems: comparison between spatial and temporal indicators. *Int. J. Bif. Chaos*, 20(2):315–321, 2010.
- [30] K.R. Elder, J. Vinals, and M. Grant. Ordering dynamics in the two-dimensional stochastic Swift-Hohenberg equation. *Phys. Rev. Lett.*, 68(20):3024–3027, 1992.
- [31] L.C. Evans. *Partial Differential Equations*. AMS, 2002.
- [32] A. García-Ojalvo, A. Hernández-Machado, and J.M. Sancho. Effects of external noise on the Swift-Hohenberg equation. *Phys. Rev. Lett.*, 71(10):1542–1545, 1993.
- [33] J. Garcia-Ojalvo and J. Sancho. *Noise in Spatially Extended Systems*. Springer, 1999.
- [34] D.I. Goldman, J.B. Swift, and H.L. Swinney. Noise, coherent fluctuations, and the onset of order in an oscillated granular fluid. *Phys. Rev. Lett.*, 92(17):174302, 2004.
- [35] B. Goldys and J.M.A.M. Van Neerven. Transition semigroups of banach space-valued Ornstein-Uhlenbeck processes. *Acta Applicandae Mathematica*, 76:283–330, 2003.
- [36] M. Gubinelli and S. Tindel. Rough evolution equations. *Ann. Probab.*, 38:1–75, 2010.
- [37] J. Guckenheimer and P. Holmes. *Nonlinear Oscillations, Dynamical Systems, and Bifurcations of Vector Fields*. Springer, New York, NY, 1983.
- [38] V. Guttal and C. Jayaprakash. Spatial variance and spatial skewness: leading indicators of regime shifts in spatial ecological systems. *Theor. Ecol.*, 2:3–12, 2009.
- [39] M. Hairer. *An Introduction to Stochastic Partial Differential Equations*. Lecture Notes, 2009. <http://www.hairer.org/notes/SPDEs.pdf>.
- [40] H. Held and T. Kleinen. Detection of climate system bifurcations by degenerate fingerprinting. *Geophys. Res. Lett.*, 31:L23207, 2004.
- [41] E. Hernández-García, M. San Miguel, and R. Toral. Noise and pattern selection in the one-dimensional Swift-Hohenberg equation. *Physica D*, 61(1):159–165, 1992.
- [42] D.J. Higham. An algorithmic introduction to numerical simulation of stochastic differential equations. *SIAM Review*, 43(3):525–546, 2001.

- [43] P.C. Hohenberg and J.B. Swift. Effects of additive noise at the onset of Rayleigh-Bénard convection. *Phys. Rev. A*, 46(8):4773–4785, 1992.
- [44] R. Hoyle. *Pattern Formation: An Introduction to Methods*. Cambridge University Press, 2006.
- [45] A. Hutt, A. Longtin, and L. Schimansky-Geier. Additive global noise delays turing bifurcations. *Phys. Rev. Lett.*, 98(23):230601, 2007.
- [46] A. Hutt, A. Longtin, and L. Schimansky-Geier. Additive noise-induced Turing transitions in spatial systems with application to neural fields and the Swift-Hohenberg equation. *Physica D*, 237(6):755–773, 2008.
- [47] S. Kéfi, M. Rietkerk, C.L. Alados, Y. Peyo, V.P. Papanastasis, A. ElAich, and P.C. de Ruiter. Spatial vegetation patterns and imminent desertification in mediterranean arid ecosystems. *Nature*, 449:213–217, 2007.
- [48] E. Kirkinis. The validity of modulation equations for extended systems with cubic nonlinearities. *Proc. R. Soc. Edinburgh A*, 122(1):85–91, 1992.
- [49] P.E. Kloeden and E. Platen. *Numerical Solution of Stochastic Differential Equations*. Springer, 2010.
- [50] C. Kuehn. A mathematical framework for critical transitions: bifurcations, fast-slow systems and stochastic dynamics. *Physica D*, 240(12):1020–1035, 2011.
- [51] C. Kuehn. Deterministic continuation of stochastic metastable equilibria via Lyapunov equations and ellipsoids. *SIAM J. Sci. Comp.*, 34(3):A1635–A1658, 2012.
- [52] C. Kuehn. A mathematical framework for critical transitions: normal forms, variance and applications. *J. Nonlinear Sci.*, 23(3):457–510, 2013.
- [53] C. Kuehn. Warning signs for wave speed transitions of noisy Fisher-KPP invasion fronts. *Theor. Ecol.*, 6(3):295–308, 2013.
- [54] C. Kuehn, E.A. Martens, and D. Romero. Critical transitions in social network activity. *J. Complex Networks*, to appear, 2014.
- [55] C. Kuehn, G. Zschaler, and T. Gross. Early warning signs for saddle-escape transitions in complex networks. *arXiv:1401.7125*, pages 1–18, 2014.
- [56] F. Kwasniok. Analysis and modelling of glacial climate transitions using simple dynamical systems. *Phil. Trans. R. Soc. A*, 371(1991):20110472, 2013.
- [57] S.J. Lade and T. Gross. Early warning signals for critical transitions: a generalized modeling approach. *PLoS Comp. Biol.*, 8:e1002360–6, 2012.

- [58] T.M. Lenton. Early warning of climate tipping points. *Nature Climate Change*, 1(4):201–209, 2011.
- [59] T.M. Lenton, H. Held, E. Kriegler, J.W. Hall, W. Lucht, S. Rahmstorf, and H.J. Schellnhuber. Tipping elements in the Earth’s climate system. *Proc. Natl. Acad. Sci. USA*, 105(6):1786–1793, 2008.
- [60] T.M. Lenton, V.N. Livina, V. Dakos, E.H. van Nes, and M. Scheffer. Early warning of climate tipping points from critical slowing down: comparing methods to improve robustness. *Phil. Trans. R. Soc. A*, 370:1185–1204, 2012.
- [61] J. Lim and B.I. Epureanu. Forecasting a class of bifurcations: theory and experiment. *Phys. Rev. E*, 83(1):016203, 2011.
- [62] V.N. Livina and T.M. Lenton. A modified method for detecting incipient bifurcations in a dynamical system. *Geophysical Research Letters*, 34:L03712, 2007.
- [63] G. Lythe. Stochastic PDEs: Domain formation in dynamic transitions. *Anales des Física, Monografías RSEF*, 4:55–63, 1998. see also arxiv:cond-mat/9808242v1.
- [64] G. Lythe and S. Habib. Stochastic PDEs: convergence to continuum? *Comput. Phys. Commun.*, 142:29–35, 2001.
- [65] C. Meisel and C. Kuehn. On spatial and temporal multilevel dynamics and scaling effects in epileptic seizures. *PLoS ONE*, 7(2):e30371, 2012.
- [66] W.W. Mohammed, D. Blömker, and K. Klepel. Modulation equation for stochastic Swift–Hohenberg equation. *SIAM J. Math. Anal.*, 45(1):14–30, 2013.
- [67] S.M. O’Regan and J.M. Drake. Theory of early warning signals of disease emergence and leading indicators of elimination. *Theor. Ecol.*, 6(3):333–357, 2013.
- [68] P.-M-Lam and D. Bagayoko. Spatiotemporal correlation of colored noise. *Phys. Rev. E*, 48(5):3267–3270, 1993.
- [69] A. Pazy. *Semigroups of Linear Operators and Applications to Partial Differential Equations*. Springer, New York, 1983.
- [70] S. Peszat and J. Zabczyk. Stochastic evolution equations with a spatially homogeneous Wiener process. *Stochastic Processes Appl.*, 72:187–204, 1997.
- [71] G. Da Prato. *Kolmogorov Equations for Stochastic PDEs*. Birkhäuser, 2004.
- [72] G. Da Prato and J. Zabczyk. *Stochastic Equations in Infinite Dimensions*. Cambridge University Press, 1992.

- [73] M. Scheffer, J. Bascompte, W.A. Brock, V. Brovkhin, S.R. Carpenter, V. Dakos, H. Held, E.H. van Nes, M. Rietkerk, and G. Sugihara. Early-warning signals for critical transitions. *Nature*, 461:53–59, 2009.
- [74] M. Scheffer and S.R. Carpenter. Catastrophic regime shifts in ecosystems: linking theory to observation. *TRENDS in Ecol. and Evol.*, 18(12):648–656, 2003.
- [75] M. Scheffer, S.R. Carpenter, T.M. Lenton, J. Bascompte, W. Brock, V. Dakos, J. van de Koppel, I.A. van de Leemput, S.A. Levin, E.H. van Nes, M. Pascual, and J. Vandermeer. Anticipating critical transitions. *Science*, 338:344–348, 2012.
- [76] D.A. Seekell, S.R. Carpenter, and M.L. Pace. Conditional heteroscedasticity as a leading indicator of ecological regime shifts. *Am. Nat.*, 178:442–451, 2011.
- [77] J. Swift and P.C. Hohenberg. Hydrodynamic fluctuations at the convective instability. *Phys. Rev. A*, 15(1):319–328, 1977.
- [78] J.M.T. Thompson and J. Sieber. Climate tipping as a noisy bifurcation: a predictive technique. *IMA J. Appl. Math.*, 76(1):27–46, 2011.
- [79] A. van Harten. On the validity of the Ginzburg-Landau equation. *J. Nonlinear Sci.*, 1(4):397–422, 1991.
- [80] E.H. van Nes and M. Scheffer. Slow recovery from perturbations as generic indicator of a nearby catastrophic shift. *Am. Nat.*, 169(6):738–747, 2007.
- [81] J.G. Venegas, T. Winkler, G. Musch, M.F. Vidal Melo, D. Layfield, N. Tgavalekos, A.J. Fischman, R.J. Callahan, G. Bellani, and R.S. Harris. Self-organized patchiness in asthma as a prelude to catastrophic shifts. *Nature*, 434:777–782, 2005.
- [82] J.M.G. Vilar and J.M. Rubi. Spatiotemporal stochastic resonance in the Swift-Hohenberg equation. *Phys. Rev. Lett.*, 78(15):2886–2889, 1997.
- [83] J. Vinals, E. Hernández-García, M. San Miguel, and R. Toral. Numerical study of the dynamical aspects of pattern selection in the stochastic Swift-Hohenberg equation in one dimension. *Phys. Rev. A*, 44(2):1123–1133, 1991.
- [84] J.B. Walsh. An introduction to stochastic partial differential equations. In *École d’été de probabilités de Saint-Flour, XIV - 1984*, volume 1180 of *Lecture Notes in Math.*, pages 265–439. Springer, 1986.